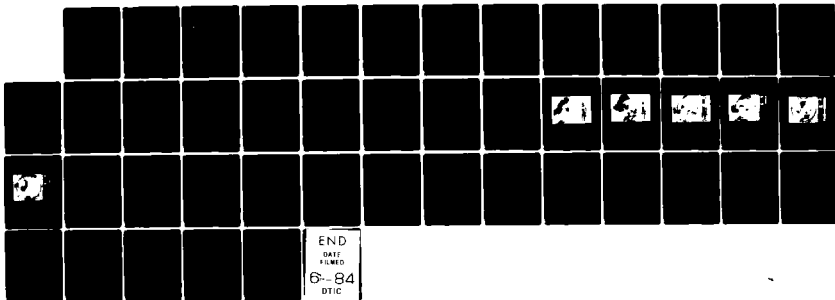
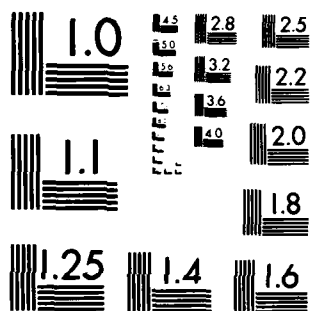


AD-A140 558 REAL TIME DIVERGENCE MEASUREMENT FROM SINGLE DOPPLER 1/1
RADAR(U) NATIONAL OCEANIC AND ATMOSPHERIC
ADMINISTRATION NORMAN OK NAT... A J KOSCIELNY 01 SEP 83
UNCLASSIFIED AFGL-TR-83-0299 ESD-2-0950 F/G 17/9 NL





MICROCOPY RESOLUTION TEST CHART
NATIONAL BUREAU OF STANDARDS-1963-A

AD-A140 558

12

AFGL-TR-83-0299

REAL TIME DIVERGENCE MEASUREMENT FROM
SINGLE DOPPLER RADAR

Albert J. Koscielny

National Oceanic and Atmospheric Administration
National Severe Storms Laboratory
1313 Halley Circle
Norman, Oklahoma 73069

Final Report
1 July - 30 September 1982

DTIC FILE COPY

1 September 1983

Approved for public release; distribution unlimited

DTIC
ELECTE
APR 26 1984
S E D

AIR FORCE GEOPHYSICS LABORATORY
AIR FORCE SYSTEMS COMMAND
UNITED STATES AIR FORCE
HANSON AFB, MASSACHUSETTS 01731


84 04 25 018

This report has been reviewed by the ESD Public Affairs Office (PA) and is releasable to the National Technical Information Service (NTIS).

This technical report has been reviewed and is approved for publication.



ALBERT C. CHMELA
Contract Manager
Ground Based Remote Sensing Branch
Atmospheric Sciences Division



KENNETH M. GLOVER
Chief, Ground Based Remote Sensing Branch
Atmospheric Sciences Division

FOR THE COMMANDER



ROBERT A. MCCLATCHEY
Director, Atmospheric Sciences Division

Qualified requestors may obtain additional copies from the Defense Technical Information Center. All others should apply to the National Technical Information Service.

If your address has changed, or if you wish to be removed from the mailing list, or if the addressee is no longer employed by your organization, please notify AFGL/DAA, Hanscom AFB, MA 01731. This will assist us in maintaining a current mailing list.

Do not return copies of this report unless contractual obligations or notices on a specific document requires that it be returned.

Unclassified

SECURITY CLASSIFICATION OF THIS PAGE

REPORT DOCUMENTATION PAGE

1a. REPORT SECURITY CLASSIFICATION Unclassified		1b. RESTRICTIVE MARKINGS N/A									
2a. SECURITY CLASSIFICATION AUTHORITY		3. DISTRIBUTION/AVAILABILITY OF REPORT Approved for public release; distribution unlimited.									
2b. DECLASSIFICATION/DOWNGRADING SCHEDULE N/A		5. MONITORING ORGANIZATION REPORT NUMBER(S) AFGL-TR-83-0299									
4. PERFORMING ORGANIZATION REPORT NUMBER(S)		7a. NAME OF MONITORING ORGANIZATION Air Force Geophysics Laboratory Hanscom AFB, MA 01731, Monitor: A. C. Chmela									
6a. NAME OF PERFORMING ORGANIZATION National Oceanic and Atmospheric Admin., Nat. Se. Storms Lab.		7b. ADDRESS (City, State and ZIP Code) Hanscom AFB, MA 01731									
6b. OFFICE SYMBOL (If applicable)		9. PROCUREMENT INSTRUMENT IDENTIFICATION NUMBER ESD 2-0950									
6c. ADDRESS (City, State and ZIP Code) 1313 Halley Circle Norman, OK 73069		10. SOURCE OF FUNDING NOS. <table border="1"><thead><tr><th>PROGRAM ELEMENT NO.</th><th>PROJECT NO.</th><th>TASK NO.</th><th>WORK UNIT NO.</th></tr></thead><tbody><tr><td>63707F</td><td>2781</td><td>278101</td><td>278101AD</td></tr></tbody></table>		PROGRAM ELEMENT NO.	PROJECT NO.	TASK NO.	WORK UNIT NO.	63707F	2781	278101	278101AD
PROGRAM ELEMENT NO.	PROJECT NO.	TASK NO.	WORK UNIT NO.								
63707F	2781	278101	278101AD								
8a. NAME OF FUNDING/SPONSORING ORGANIZATION Air Force Geophysics Laboratory		11. TITLE (Include Security Classification) Real Time Divergence Measurement from Single Doppler Radar									
8b. OFFICE SYMBOL (If applicable) LYR		12. PERSONAL AUTHOR(S) Albert J. Koscielny									
8c. ADDRESS (City, State and ZIP Code) Hanscom AFB, MA 01731		13a. TYPE OF REPORT Final									
13b. TIME COVERED 82 FROM 1 July TO 30 Sep		14. DATE OF REPORT (Yr., Mo., Day) 83 September 1									
15. PAGE COUNT 44		16. SUPPLEMENTARY NOTATION									
17. COSATI CODES <table border="1"><thead><tr><th>FIELD</th><th>GROUP</th><th>SUB. GR.</th></tr></thead><tbody><tr><td>04</td><td>0402</td><td></td></tr></tbody></table>		FIELD	GROUP	SUB. GR.	04	0402		18. SUBJECT TERMS (Continue on reverse if necessary and identify by block number) Doppler weather radar Linear wind analysis Mesoscale convergence			
FIELD	GROUP	SUB. GR.									
04	0402										
19. ABSTRACT (Continue on reverse if necessary and identify by block number) Mesoscale convergence is thought to influence development of convective storms. Convergence can be measured with a single Doppler radar if the wind field is approximately spatially linear. The algorithm for measuring convergence from radial velocities is presented. The algorithm is feasible for real time application to two elevation angles of a tilt sequence of five or more elevation angles. This convergence measurement technique is applied to widespread convective precipitation in central Oklahoma on April 9, 1978. Analysis results and the suitability of the spatial linearity assumption are discussed.											
20. DISTRIBUTION/AVAILABILITY OF ABSTRACT UNCLASSIFIED/UNLIMITED <input type="checkbox"/> SAME AS RPT. <input checked="" type="checkbox"/> DTIC USERS <input type="checkbox"/>		21. ABSTRACT SECURITY CLASSIFICATION Unclassified									
22a. NAME OF RESPONSIBLE INDIVIDUAL A. C. Chmela		22b. TELEPHONE NUMBER (Include Area Code) 617-861-4405									
		22c. OFFICE SYMBOL AFGL/LYR									

DD FORM 1473, 83 APR

EDITION OF 1 JAN 73 IS OBSOLETE.

Unclassified

SECURITY CLASSIFICATION OF THIS PAGE

Acknowledgements

My thanks to Evelyn Horwitz for typing the manuscript, Joan Kimpel for drafting the figures, and Bob Goldsmith and Charles Clark for the photographic work.

Accession For	
NTIS GRA&I	<input checked="" type="checkbox"/>
DTIC TAB	<input type="checkbox"/>
Unannounced	<input type="checkbox"/>
Justification	
By _____	
Distribution/	
Availability Codes	
Dist	Avail and/or Special
A-1	



Contents

1. INTRODUCTION	6
2. LINEAR WIND FIELD MEASUREMENT	7
2.1 Divergence Measurement	8
2.2 Real Time Expediencies	9
2.3 Scales of Motion Represented by the Linear Wind Analysis	11
3. A REAL TIME DIVERGENCE MEASUREMENT PROGRAM	11
3.1 DIVDATA	13
3.1.1 Velocity Unfolding	13
3.1.2 Editing	13
3.1.3 Storing Averaged Velocities	15
3.1.4 DIVDATA Termination	15
3.2 DIVLWA	15
3.2.1 Linear Wind Analysis	15
3.2.2 Analysis Results	15
3.3 Display Programs	15
4. AN APPLICATION TO WIDESPREAD PRECIPITATION DATA	19
4.1 Meteorological Conditions	19
4.2 Divergence Measurements	20
4.3 Linearity of the Velocity Fields	31
5. SUMMARY AND CONCLUSIONS	34
REFERENCES	36
APPENDIX A: Effects of Applying a Linear Approximation to Sinusoidal Phenomena	38
APPENDIX B: Documentation for RLTDIV Subroutine	42

Illustrations

1.	Division of data into analysis volumes. Analysis volumes are referenced by center azimuth ϕ_0 and center range r_0 (shown only for the first volume).	10
2.	Flow chart for DIVERGE program.	12
3.	Flow chart for DIVDATA segment.	14
4.	Flow chart for DIVLWA segment.	16
5.	Flow chart for DIVPRT and DIVPLT display programs.	18
6.	Norman Doppler reflectivities in dBZ for 1732 CST on April 9, 1978.	21
7.	Reflectivities for 1847 CST.	22
8.	Radial velocities (m s^{-1}) for elevations 0.5° (a) and 0.9° (b) for 1732 CST.	23
9.	Radial velocities (m s^{-1}) for 1847 CST.	25
10.	Divergence measured by the linear wind analysis for 1732 CST. Range marks are at 40 km intervals.	30
11.	Divergence for 1847 CST.	32
12.	Radial velocity data for an analysis volume at 265° , 66.6 km for 1732. Measured radial velocity is plotted against the linearly modeled radial velocity, denoted by + . Solid line is a perfect linear relationship.	33
13.	Same as Figure 12 but for 285° , 42.3 km.	35
A.1	Linear least squares approximation of a cosine wave.	39
A.2	Response of the least squares slope estimate to a sine wave. Wave fraction is the ratio of the fitting interval (X in Figure A.1) to the wavelength L.	41

Tables

1a.	Linear Wind Analysis Results for 1732 CST, April 9, 1978.	27
1b.	Linear Wind Analysis Results for 1847 CST, April 9, 1978.	28

REAL TIME DIVERGENCE MEASUREMENT FROM SINGLE DOPPLER RADAR

1. INTRODUCTION

Mesoscale convergence is generally thought to influence subsequent convective development and should provide a valuable forecast tool.¹ Chen and Orville² conclude that knowledge of the mesoscale convergence field will be needed to forecast cloud scale convection for three to six hours in advance. In previous analyses of mesoscale convergence, measurements have been made from a surface and/or sounding network^{3,4} or from multiple Doppler radar observations.⁵ Because these approaches require elaborate coordination or extensive computation, they are not now convenient for real time application.

Divergence fields can be measured with a single Doppler radar if some simplifying assumptions about the temporal and spatial variation of the wind field

(Due to the large number of references cited above, they will not be listed here. See References, page 36).

can be made. A number of studies have been made using various assumptions, as summarized by Waldteufel and Corbin.⁶ (For simplicity, divergence will be used hereafter with the understanding that negative values are important.) Based on these studies, the most viable assumptions for divergence measurement appear to be that of a time invariant (over the scanning period), spatially linear wind field.

This report presents an algorithm for mesoscale divergence measurement with a single Doppler radar based on these assumptions. The theoretical development, presented by Koscielny *et al.*⁷ is summarized in section 2. A Fortran implementation of this algorithm is discussed in section 3. The results of an application to a widespread convective precipitation case is presented in section 4.

2. LINEAR WIND FIELD MEASUREMENT

The measurement of the components and/or derivatives of the linear wind field from radial velocities is discussed by Koscielny *et al.*⁷ The measured radial velocity v_r can be modeled by the linear regression equation

$$v_r = P_m K_m + \epsilon \quad (1)$$

where P_m is a row vector of m regressor variables that are functions of range r , azimuth ϕ , and elevation θ_e ; K_m is a column vector of m corresponding parameters of the linear wind field. The measured v_r , a reflectivity weighted mean of radial velocities within the radar's resolution volume, can contain errors due to nonuniform reflectivity, measurement error, targets such as hydrometeors moving relative to the wind, and nonlinearity of the wind.

-
6. Waldteufel, P., and Corbin, H. (1979) On the analysis of single Doppler data. *J. Appl. Meteor.*, 18, pp 532-542.
 7. Koscielny, A.J., Doviak, R.J., and Rabin, R. (1982) Statistical consideration in the estimation of divergence from single Doppler radar and application to prestorm boundary layer observations. *J. Appl. Meteor.*, 21, pp 199-210.

Collecting n measurements into a column vector V_n , a least squares estimate of K_m can be computed by

$$\hat{K}_m = [P_{nm}^t P_{nm}]^{-1} [P_{nm}^t V_n] \quad (2)$$

where t indicates transpose and P_{nm}^t is an $n \times m$ matrix of the regressor variables corresponding to the n radial velocity measurements in V_n . The covariances of the estimate \hat{K}_m about K_m are given by

$$C_{mm} = [P_{nm}^t P_{nm}]^{-1} \sigma_\epsilon^2 \quad (3)$$

where σ_ϵ^2 is the variance of ϵ . σ_ϵ^2 can be estimated by the residual sum of squares

$$s^2 = (n-m)^{-1} E_n^t E_n \quad (4)$$

where

$$E_n = [V_n - P_{nm}^t K_m] .$$

A linear wind field analysis is done by fitting (1) to a suitably chosen set of radial velocities. This set is usually chosen to lie within a spatial volume termed the analysis volume. The shape of the analysis volume has not been specified but the parameters included in K_m will usually place some restrictions on it so they can be estimated by (2) with sufficiently small errors.

2.1 DIVERGENCE MEASUREMENT

For divergence measurements, u_x and v_y are included, where, for example, u_x is the partial derivative of u in the x direction. To estimate u_x and v_y with reasonable accuracy, the analysis volume should cover at least 20 km in both the x and y directions. If data for a constant elevation angle is used, the radial velocity will contain variations due to the vertical gradients of the linear wind field. Thus the analysis volume must include data for at least two elevation

angles so the vertical variations of wind can be measured. Seven parameters (u_0 , u_x , u_z , v_0 , v_y , v_z , $u_y + v_x$) will be included in K_m .

Four parameters of the linear wind field (w_0 , w_x , w_y , w_z) have been neglected. For low elevation angles ($<1^\circ$ – 2°) the bias in the divergence estimate is negligible ($<10^{-5} \text{ s}^{-1}$) if $w_0 < 1 \text{ m s}^{-1}$; w_x , $w_y < 10^{-2} \text{ s}^{-1}$; $w_z < 10^{-1} \text{ s}^{-1}$. (However, estimates of the other parameters, such as u_0 and v_0 , could be significantly biased by neglected vertical terms.)

2.2 REAL TIME EXPEDIENCIES

The algorithm is designed for application to two low elevation angles. Since radar observations are usually made on a tilt sequence of several elevation angles, the algorithm would be executed at about ten minute intervals. To keep execution time to less than ten minutes, two simplifications are used.

2.2.1 ANALYSIS VOLUME DESIGN

As noted earlier, the shape of the analysis volume is somewhat arbitrary. Two elevation angles are needed and some evaluations of (3) with nominal values show that it should be at least 30° in azimuthal width. For this application, data is divided into adjustable sectors of azimuthal width $\Delta\phi$ and range length Δr , as shown in Figure 1. This simplification (i.e., a rectangular volume in polar coordinates) minimizes the data management needed to collect the radial velocities for a given analysis volume.

2.2.2 RANGE INTERVAL AVERAGING

A second simplification is the averaging of radial velocities over short range intervals. In computing the least squares estimates (2), m regressors P_m are evaluated for each of the n radial velocities. The regressors are sine cosine products. For a typical case of an analysis volume $30^\circ \times 30 \text{ km}$ with 2 elevations, a radial spacing of 1° and a gate spacing of 150 m, $n \approx 12000$. Most of the computation in evaluating (2) is for the regressors.

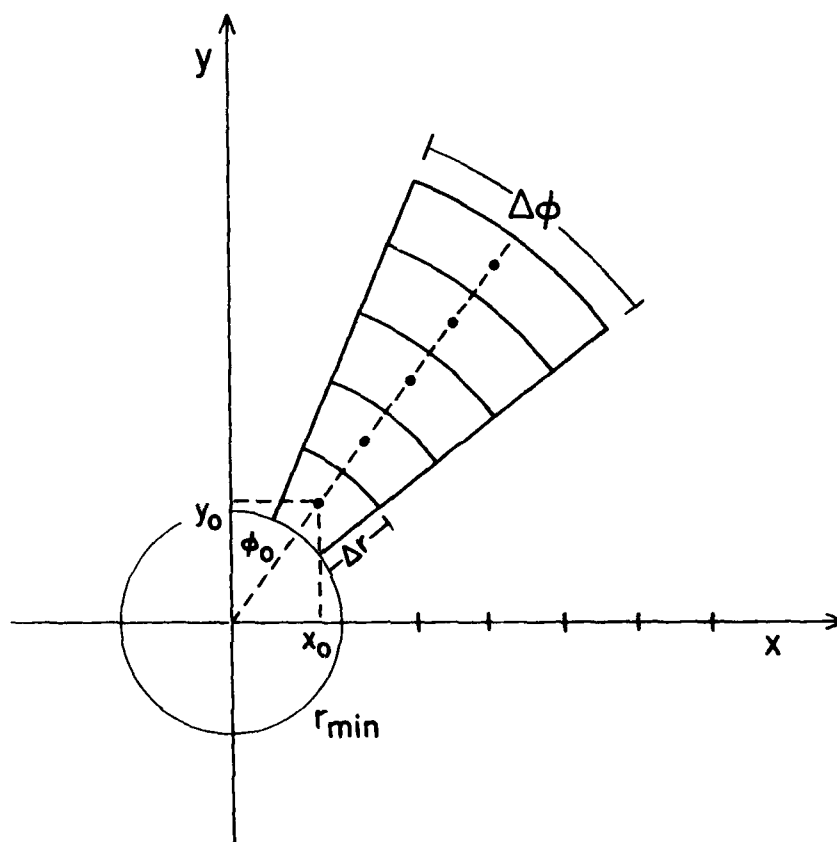


Figure 1. Division of data into analysis volumes. Analysis volumes are referenced by center azimuth ϕ_0 and center range r_0 (shown only for the first volume).

However, the radial velocity for a linear wind field is, except for the earth curvature term, a linear function of range. For short range intervals (~ 10 km) the curvature term can be neglected and the radial velocities averaged to give a value representative at the midpoint. Linear wind analysis of the averaged data will give results nearly identical to those for the original data.

2.3 SCALES OF MOTION REPRESENTED BY THE LINEAR WIND ANALYSIS

This divergence measurement is made assuming constant divergence over the analysis volume. The atmosphere, however, contains all scales of motion and the constant divergence assumption is accurate for phenomena large compared to the dimensions of the analysis volume. For the present application, this would be scales of 200 km or longer.

The representation of a sinusoidal divergence field by a constant is considered in detail in Appendix A. It is shown that the divergence values are increasingly attenuated with shorter wavelengths of a sinusoidal field. Because the sectors are of constant azimuthal width, the minimum scale depends on range. Thus the linear wind analysis accurately measures the larger scale (≥ 200 km) divergence but attenuates scales between about 40 km and 200 km.

3. A REAL TIME DIVERGENCE MEASUREMENT PROGRAM

DIVERGE is a Fortran implementation of the divergence measurement algorithm. DIVERGE can be divided into three consecutive segments:

- (1) DIVDATA - collect, edit, average, and store radial velocity data for two low elevation PPI's,
- (2) DIVLWA - divergence measurements through linear wind analysis for small sectors,
- (3) DIVPLT, DIVPRT - plot and/or print analysis results.

Figure 2 shows the flow of data through the DIVERGE program.

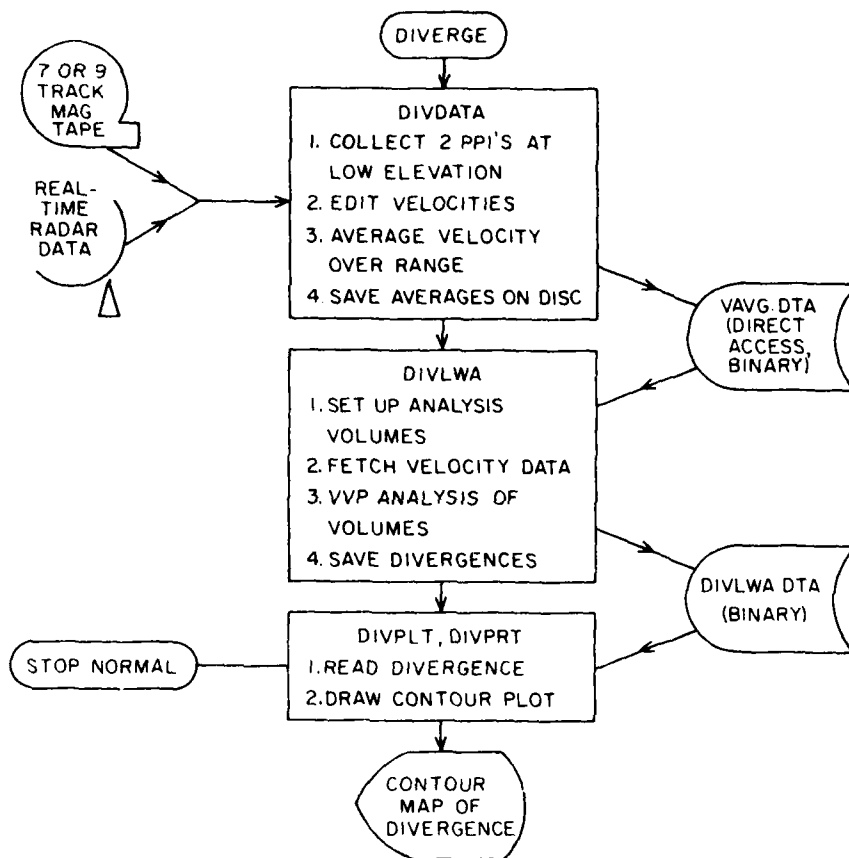


Figure 2. Flow chart for DIVERGE program.

3.1 DIVDATA

The linear wind analysis uses least squares estimation and therefore requires unfolded and edited radial velocity data. Much of the DIVDATA routine depends on specifics of the application and the following description of the routine for processing NSSL's Norman Doppler data is intended to provide an example. A flow chart of DIVDATA is shown in Figure 3.

3.1.1 VELOCITY UNFOLDING

There are several velocity unfolding techniques, but none are completely adequate. For programming simplicity DIVDATA uses a technique described by Hennington,⁸ which uses an independent estimate of a uniform wind speed and direction. The wind estimate is usually made from a subjective interpretation of the radial velocity display.

3.1.2 EDITING

DIVDATA uses spatial coherency of the radial velocities as a basis for editing. The radial velocities for the range averaging interval are passed to a subroutine EDMEAN. EDMEAN computes a histogram of these velocities. Values at zero are considered ground clutter and ignored. The nonzero mode of the histogram is a first guess of the average radial velocity. Velocities too far from this average value are discarded as being outliers and the average of the remaining data computed. A check for random velocities (noise) is made by requiring that the frequency count for the mode be greater than some specified minimum. If EDMEAN is unable to compute an average, it returns a missing value code. (This editing procedure is still being developed and the values of the various criteria are not firmly established.) The editing and averaging is thus combined.

8. Hennington, L. (1981) Reducing the effects of Doppler radar ambiguities. J. Appl. Meteor., 20, pp 1543-1546.

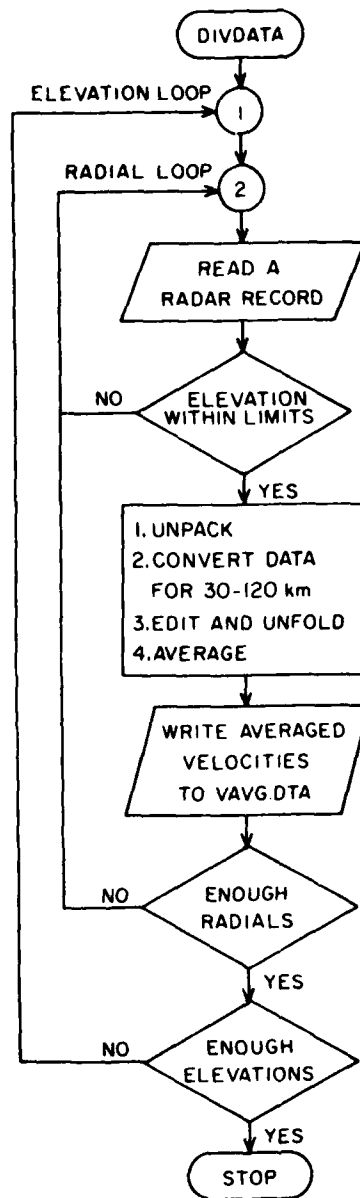


Figure 3. Flow chart for DIVDATA segment.

3.1.3 STORING AVERAGED VELOCITIES

The averaged radial velocities for a given radial are stored on disc for the analysis routine. In the current setup, a 1° azimuthal spacing is assumed. To facilitate the later data access by DIVLWA, a direct access file (shown in Figure 2 as VAVG.DTA) is used. 720 records are allocated and the azimuth angle is truncated to give the record number. The lower elevation PPI is stored in records 1-360 and the upper one in records 361-720. Because there may not be any data for some of the azimuths, the file is initialized to a missing value code. The azimuth spacing is never exactly 1° , so occasionally, a record will be overwritten.

3.1.4 DIVDATA TERMINATION

DIVDATA uses a radial counter to determine when data collection is complete. On completion, DIVDATA closes the output file and terminates.

3.2 DIVLWA

The analysis routine has four functions:

1. set up overlapping analysis volumes,
2. collect the appropriate average data,
3. perform a linear wind analysis,
4. store the divergence measurements and some quality control statistics [standard error of estimate, root mean square error about the linear model (rms)],

as shown in the flow chart in Figure 4.

The first two functions are easily done since the input data is the direct access file VAVG.DTA. Once the sector limits are specified, data record limits are known and the appropriate data read using direct access read.

3.2.1 LINEAR WIND ANALYSIS

Before the linear wind analysis, DIVLWA checks if there is adequate data for an accurate analysis. The actual spread of azimuths and the number of good data are computed. If these are above preset minimums is the analysis done.

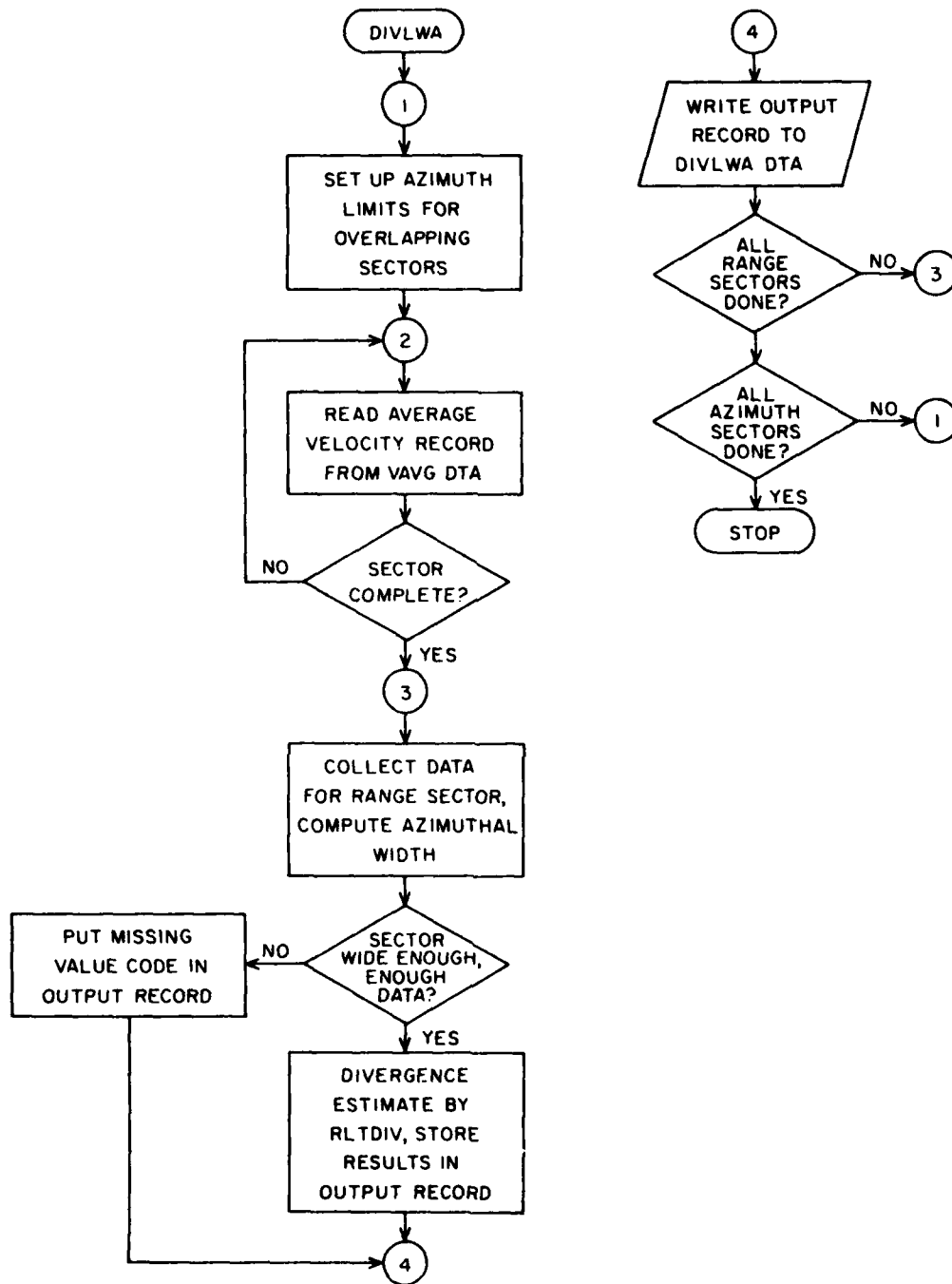


Figure 4. Flow chart for DIVLWA segment.

The linear wind analysis is done by the subroutine RLTDIV. RLTDIV is documented internally by comments; a flow chart and list of variables is in Appendix B. RLTDIV contains only straightforward computation for evaluating (2). The only error is for a zero determinant, which generally indicates a serious problem with the input data to RLTDIV (such as all azimuth angles being identical).

3.2. ANALYSIS RESULTS

The number of data used, estimated linear wind parameters, rms, and the divergence and its standard error are written to a print file which can be printed with a PRINT DIVLWA.PRT. The divergence, its standard error, and the rms are written to a data file (DIVLWA.SAV) for use by the display module.

3.3 DISPLAY PROGRAMS

Two programs are available for displaying the results of the linear wind analysis. DIVPRT is a rather unsophisticated routine that prints a contour map on the line printer. The divergence estimates, on a polar grid centered at the radar, are interpolated to a 21 x 21 rectangular array using the bivariate interpolation routine IDSFFT described by Akima.⁹ The inscribed circle in the array is then contoured.

DIVPLT uses the NCAR graphics software described by McArthur¹⁰ to draw a contour map. The divergence measurements are read into an array and thus represent gridded value on a polar coordinate system. A missing value indicator is used so the contouring routine CONREC does not draw contours where divergence measurements could not be made. The contour coordinates are then transformed from polar to rectangular as described by McArthur¹⁰ (Appendix B). The NCAR

9. Akima, H. (1978) A method of bivariate interpolation and smooth surface fitting for irregularly distributed data points. ACM, Trans. on Math. Software, 4, pp 148-159.

10. McArthur, G.R. (1981) The SCD graphics utilities, NCAR Technical Note TN/166 + IA.

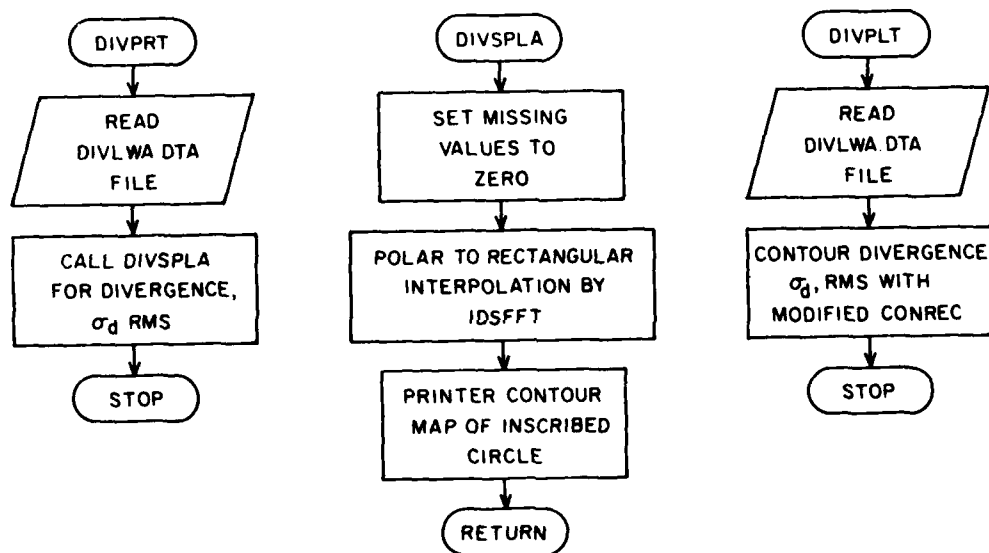


Figure 5. Flow chart for DIVPRT and DIVPLT display programs.

graphics software writes to a metacode file that can be directed to a variety of plotting devices. The flow chart for DIVPRT and DIVPLT are shown in Figure 5.

4. AN APPLICATION TO WIDESPREAD PRECIPITATION DATA

An attempt was made to test DIVERGE on a stratiform precipitation case from the CHILL radar for January 22, 1982. However, the radial velocity data contained a large portion of bad values, apparently due to a bit hang problem in the pulse pair processor. Because the anticipated rewards did not seem commensurate with the rehabilitation effort for this data, a data set collected with the Norman Doppler radar for April 9, 1978, was used for testing.

The meteorological conditions for April 9 were widespread convective precipitation. Although the linearity assumption would apply better to a stratiform precipitation case, this data will be adequate for testing. In addition, a technique for examining the appropriateness of the linearity assumption can be illustrated on this data.

4.1 METEOROLOGICAL CONDITIONS

The synoptic situation on April 9 was conducive to thunderstorm development. The presence of a surface boundary in western Oklahoma, adequate low level moisture, diffluence at 500 mb, and the approach of a moderate short wave were the factors favorable for severe storm development. However, weak meridional winds and moisture at 700 mb decreased the possibility of tornadic storms.

Joint Doppler Operational Program¹¹ operations began at 1400 CST, after convection had begun. During the afternoon and early evening, there were high winds and hail in western Oklahoma but no confirmed tornadoes. Much of the severe weather was due to a large thunderstorm to the west of Norman. It had been tracked by JDOP personnel from 1407 CST. Movement was eastward at about

11. JDOP Staff (1979) Final report on the Joint Doppler Operational Project (JDOP), 1976-1978. NOAA Tech. Memo. ERL NSSL-86, 84 pp.

40 km hr⁻¹ (11 m s⁻¹). In its later stages, this storm had a large scale circulation signature. The storm weakened considerably after 1800 CST and the severe weather advisories were discontinued at 1847 CST.

The times selected for testing the DIVERGE program are 1732 CST and 1847 CST. The reflectivity fields for these times are shown in Figures 6 and 7 for a 0.5° elevation and the radial velocity fields in Figures 8 and 9 for 0.5° and 0.9° elevations. At 1732 the large thunderstorm is located at about 260°/95 km from Norman and at 1847 has moved to 270°/40 km. There is adequate signal for velocity measurement over about half the PPI (to 115 km) at these times. The radial velocity fields show the wind is generally from the south. The large circulation signature associated with the thunderstorm can be seen at both times (1732 and 1847) and both elevation angles.

4.2 DIVERGENCE MEASUREMENTS

Data at the elevation angles 0.5° and 0.9° were selected for analysis. The tilt sequences contain a lower elevation angle (0.2°) but it is unsuitable because of beam blockage. The radial velocity data between 30 km and 115 km (138 km for 1732 CST) were edited and averaged by the EDMEAN subroutine as described in section 3.1.2. The number of range gates averaged was 45, corresponding to a range interval of 6.75 km (8.1 km for 1732). The interval for the histogram analysis was 2.0 m s⁻¹; minimum number of good data 5; no minimum count for the mode. Visual inspection of the velocity data showed no folded velocities so no unfolding was done. The signal to noise threshold was 5 dB and the relative suppression (for expanded mode) was 10 dB.⁸ The averaged values, along with some housekeeping information were stored in the direct access files VAVG4091.SAV and VAVG4092.SAV.

The linear wind analysis program DIVLWA was run using these files as input data. The divergence measurements are shown in Figures 10 and 11 for 1732 and 1847, respectively. Values of divergence, the standard error of the measurement, and the root mean square (rms) of the residuals are given in Table 1.

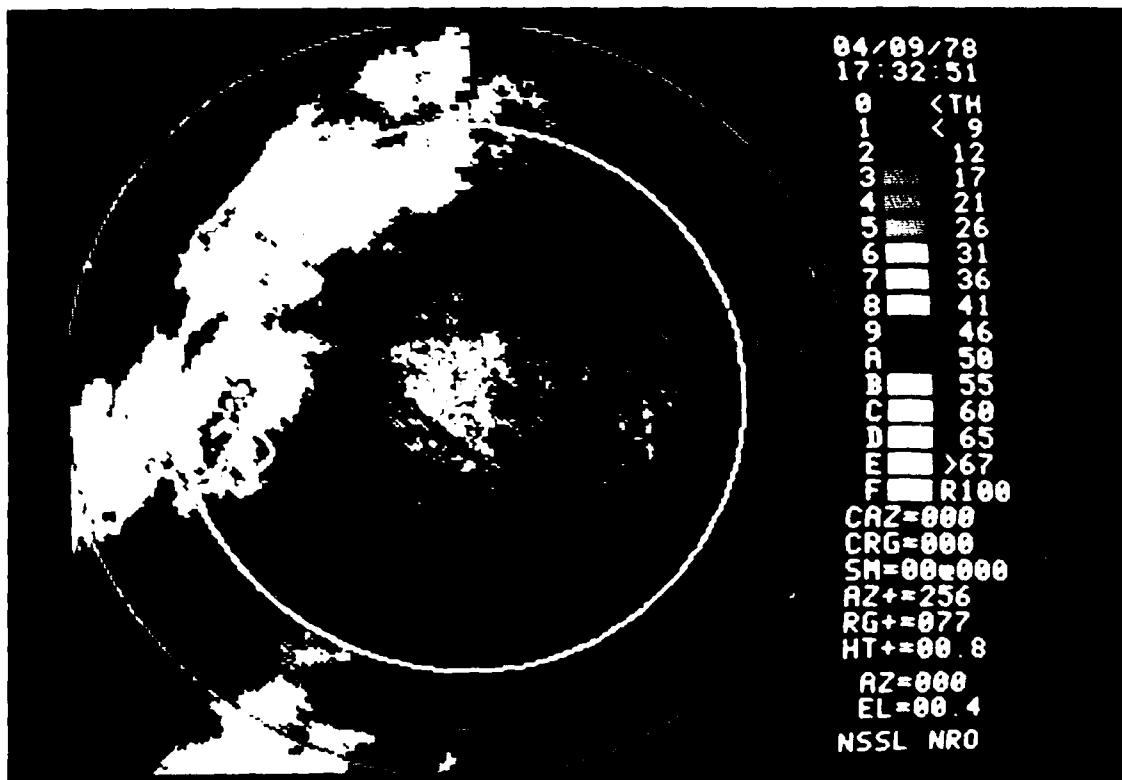


Figure 6. Note in lander reflectivities in GR7
for 17:32:51 on April 9, 1978.

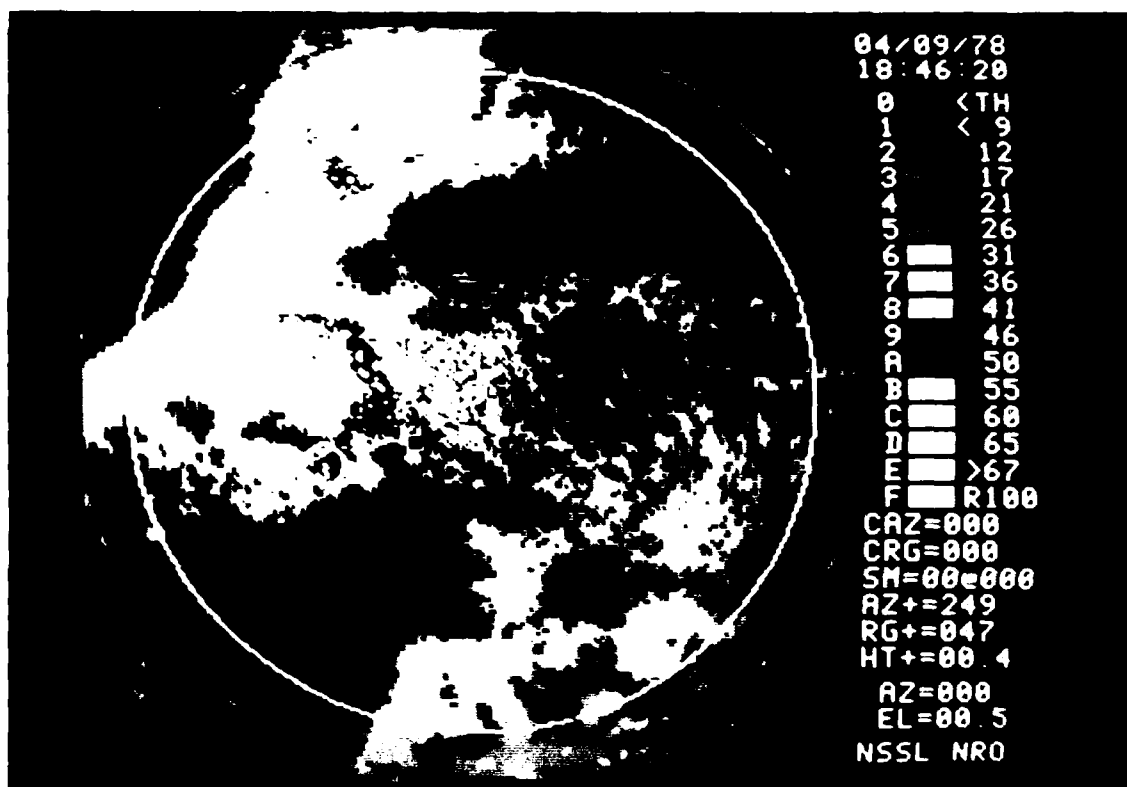


Figure 7. Reflectivities for 1847 CST.

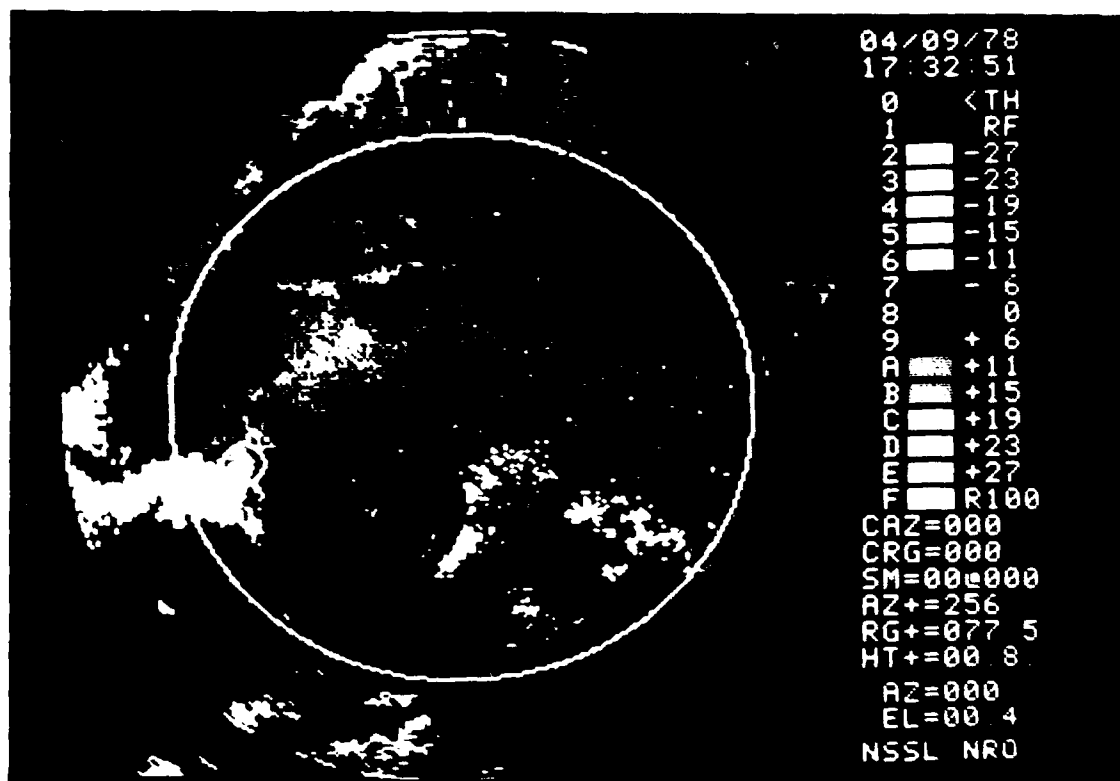


Figure 8. Radial velocities (a) for elevations 0.5° and 0.90° (b) for 1732 CST.

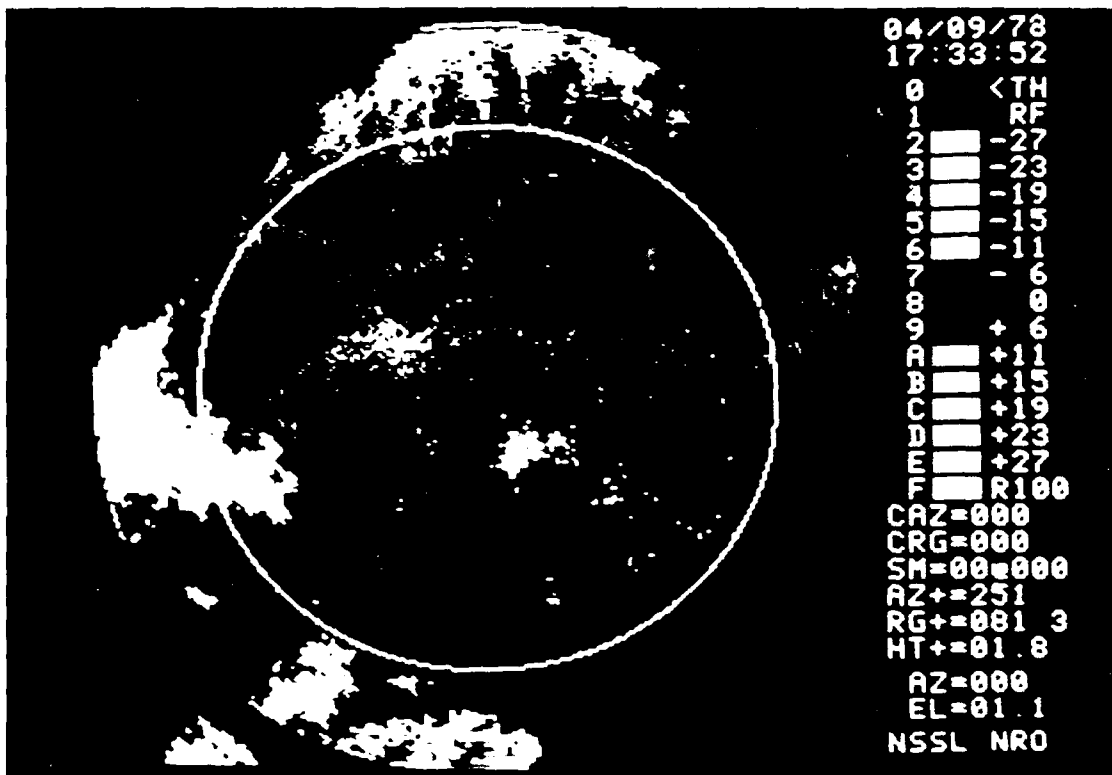


Figure 3b.

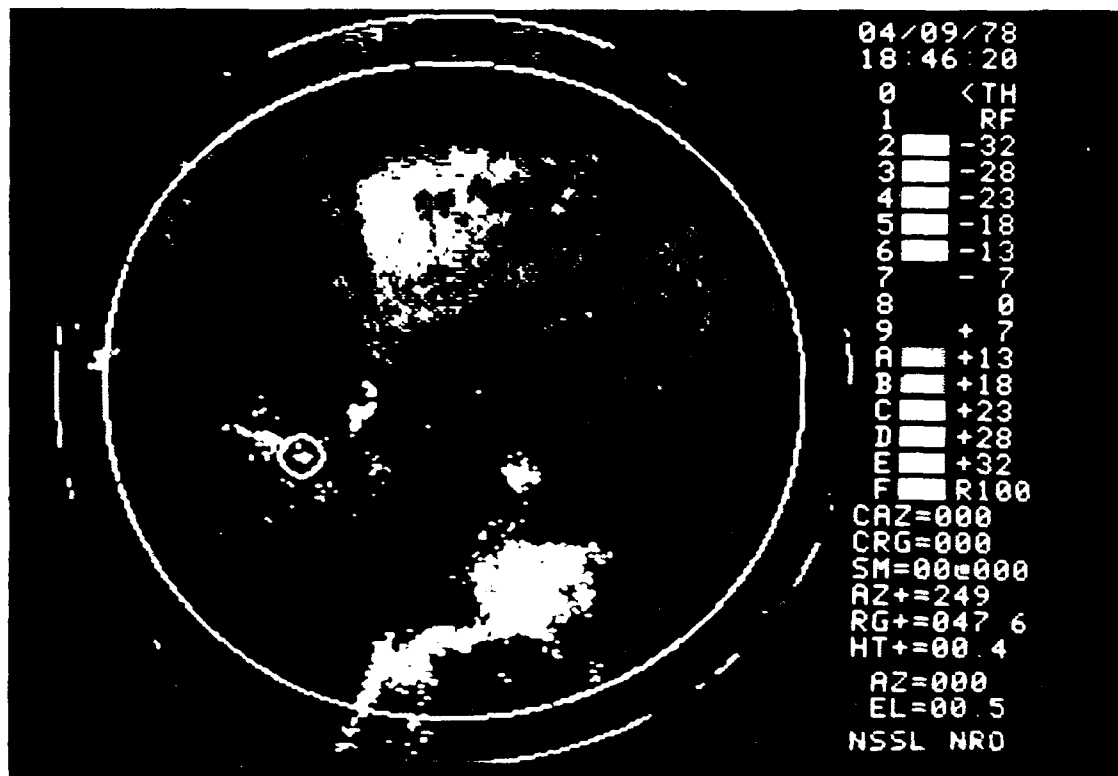


Figure 9. Radial velocities (km s^{-1}) for 1947 GST.

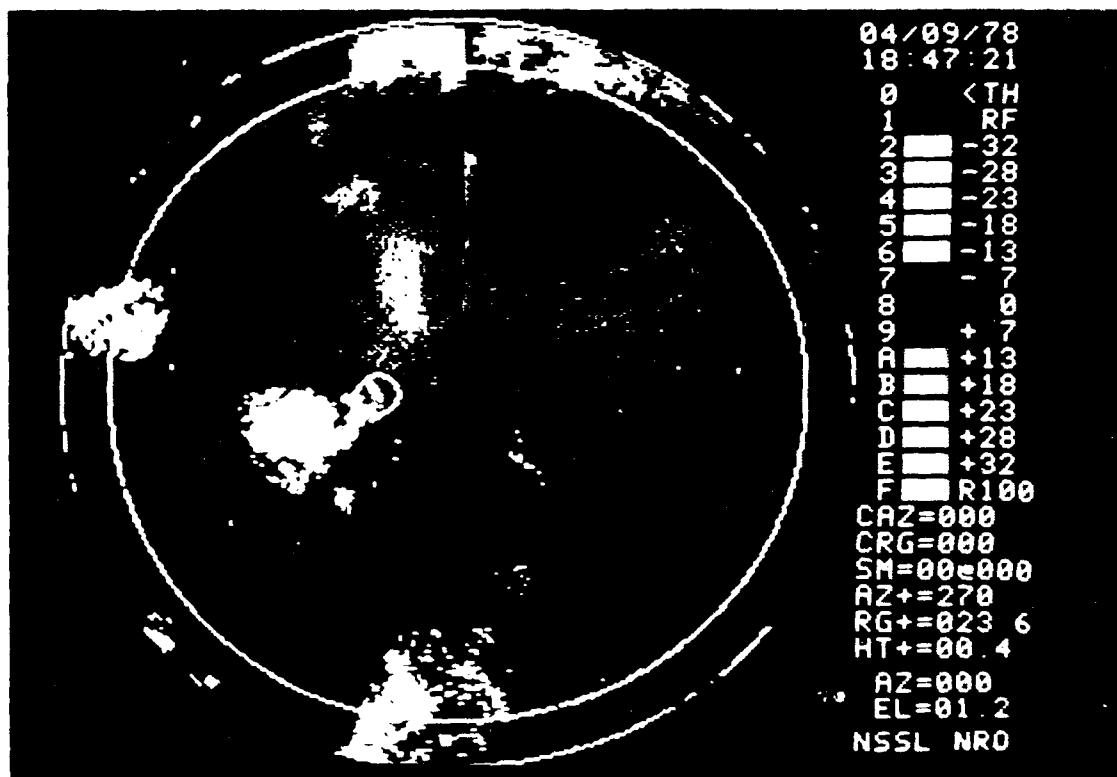


Figure 10.

Table 1a. Linear Wind Analysis Results for 1732 CST, April 9, 1978.					
Center of Analysis Volume			Divergence (10^{-5} s^{-1})	σ_d (10^{-5} s^{-1})	RMS (m s^{-1})
Azimuth degrees)	Range (km)	Elevation Angle (degrees)			
75	42.3	0.6	-3	14	0.99
85	66.6	0.6	2	9	0.81
95	42.3	0.6	39	13	0.90
95	66.6	0.6	30	7	0.83
105	66.6	0.6	9	5	0.82
115	66.6	0.6	8	6	0.64
265	66.6	0.6	-185	20	3.31
265	90.8	0.6	-159	14	3.46
265	115.1	0.6	26	7	1.75
275	66.6	0.6	-17	5	1.00
275	90.8	0.6	-15	10	2.50
275	115.1	0.6	-39	13	1.89
285	42.3	0.6	21	3	0.36
285	66.6	0.6	21	6	1.13
285	90.8	0.6	0	8	1.88
285	115.1	0.6	-47	30	2.25
295	42.3	0.6	-4	13	0.75
295	66.6	0.6	-28	5	0.96
295	90.8	0.6	12	6	1.51
305	42.3	0.6	-112	17	1.04
305	66.6	0.6	-23	5	0.98
305	90.8	0.6	-8	5	1.29
315	66.6	0.6	-1	7	1.21
315	90.8	0.6	19	7	1.66
315	115.1	0.6	30	40	2.25
325	66.6	0.6	-13	8	1.36
325	90.8	0.6	67	7	1.56
325	115.1	0.6	-17	17	1.88
335	66.6	0.6	-13	10	1.76
335	90.8	0.6	11	7	1.72
335	115.1	0.6	12	7	1.51
345	66.6	0.6	10	13	1.83
345	90.8	0.6	3	8	1.87
345	115.1	0.6	1	5	1.38
355	66.6	0.6	50	16	2.05
355	90.8	0.6	58	10	2.24
355	115.1	0.6	16	5	1.30
365	90.8	0.6	61	12	2.30
365	115.1	0.6	28	5	1.19

Table 1b. Linear Wind Analysis Results for 1847 CST, April 9, 1978.

Center of Analysis Volume			Divergence (10^{-5} s^{-1})	σ_d (10^{-5} s^{-1})	RMS (m s^{-1})
Azimuth degrees)	Range (km)	Elevation Angle (degrees)			
15	40.1	0.8	4	15	1.13
15	80.6	0.8	-13	15	2.62
15	100.8	0.8	62	12	1.63
25	40.1	0.8	-3	15	1.04
35	40.1	0.8	18	12	0.97
45	40.1	0.8	38	7	0.73
55	40.1	0.8	-2	8	0.84
55	60.4	0.8	12	7	0.90
65	40.1	0.8	-9	7	0.78
65	60.4	0.8	-4	5	0.75
65	80.6	0.8	-2	6	0.57
75	40.1	0.8	24	9	0.93
75	60.4	0.8	-4	7	1.07
75	80.6	0.8	-3	5	0.56
85	40.1	0.8	-10	8	0.85
85	60.4	0.8	20	6	1.04
85	80.6	0.8	-6	4	0.69
95	40.1	0.8	29	8	0.88
95	60.4	0.8	25	6	1.00
95	80.6	0.8	-22	5	0.84
105	40.1	0.8	5	7	0.76
105	60.4	0.8	-19	5	0.91
105	80.6	0.8	-40	5	0.93
105	100.8	0.8	-4	7	1.39
115	40.1	0.8	30	6	0.64
115	60.4	0.8	35	5	0.81
115	80.6	0.8	12	5	1.03
115	100.8	0.8	-14	9	1.49
125	40.1	0.8	44	5	0.51
125	60.4	0.8	-0	5	0.82
125	80.6	0.8	-19	5	1.03
125	100.8	0.8	19	7	1.22
135	40.1	0.8	9	5	0.53
135	60.4	0.8	-25	4	0.70
135	80.6	0.8	-1	3	0.81
135	100.8	0.8	16	4	0.82
145	40.1	0.8	27	10	0.93
145	60.4	0.8	-25	5	0.74
145	80.6	0.8	-14	3	0.64
145	100.8	0.8	3	3	0.86
155	40.1	0.8	-25	17	1.28
155	60.4	0.8	-2	8	0.93
155	80.6	0.8	7	4	0.81
155	100.8	0.8	0	4	1.00
165	80.6	0.8	-1	8	1.51
165	100.8	0.8	-19	4	1.04
175	80.6	0.8	-34	12	2.42
175	100.8	0.8	23	4	0.99

Table 1b (cont.). Linear Wind Analysis Results for 1847 CST,
April 9, 1978.

Center of Analysis Volume					
Azimuth degrees)	Range (km)	Elevation Angle (degrees)	Divergence (10^{-5} s^{-1})	(10^{-5} d^{-1})	RMS (m s^{-1})
235	40.1	0.8	-24	23	1.72
245	40.1	0.8	11	14	1.66
245	60.4	0.8	48	9	1.03
255	40.1	0.8	52	11	1.29
255	60.4	0.8	72	7	1.16
255	80.6	0.8	22	6	0.86
265	40.1	0.8	126	16	1.92
265	60.4	0.8	70	9	1.50
265	80.6	0.8	30	5	1.14
265	100.8	0.8	-8	9	1.97
275	40.1	0.8	58	18	2.03
275	60.4	0.8	36	10	1.62
275	80.6	0.8	66	8	1.60
275	100.8	0.8	80	13	2.15
285	40.1	0.8	-61	18	1.93
285	60.4	0.8	-51	10	1.62
285	80.6	0.8	5	10	1.98
285	100.8	0.8	58	25	2.02
295	40.1	0.8	-89	13	1.39
295	60.4	0.8	-35	9	1.41
295	80.6	0.8	7	9	1.86
305	40.1	0.8	-68	12	1.19
305	60.4	0.8	-22	7	1.16
305	80.6	0.8	-11	7	1.47
315	40.1	0.8	35	17	1.71
315	60.4	0.8	8	8	1.17
315	80.6	0.8	-13	7	1.48
315	100.8	0.8	-37	23	1.99
325	40.1	0.8	31	16	1.74
325	60.4	0.8	10	12	2.03
325	80.6	0.8	-44	9	1.91
325	100.8	0.8	21	14	2.32
335	40.1	0.8	-93	14	1.20
335	60.4	0.8	-28	11	1.99
335	80.6	0.8	-31	10	2.18
335	100.8	0.8	61	10	2.55
345	40.1	0.8	4	12	1.24
345	60.4	0.8	-33	14	2.01
345	80.6	0.8	-7	11	2.44
345	100.8	0.8	-9	10	2.61
355	40.1	0.8	107	17	1.43
355	60.4	0.8	19	7	0.91
355	80.6	0.8	-43	12	2.47
355	100.8	0.8	-10	10	2.38
365	40.1	0.8	-13	26	1.46
365	80.6	0.8	1	12	2.48
365	100.8	0.8	67	8	1.52

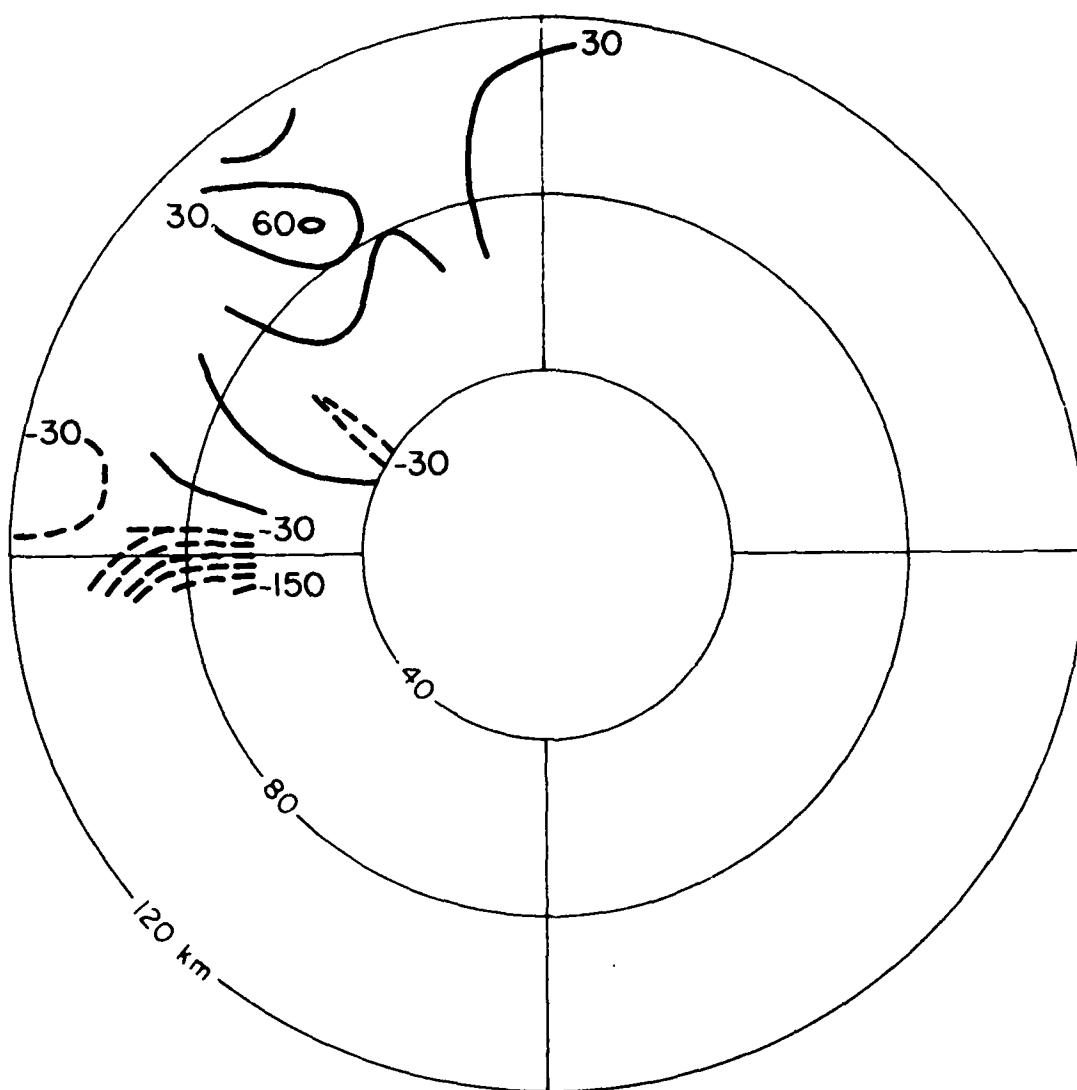


Figure 10. Divergence measured by the linear wind analysis for 1732 CST.

The analysis for 1732 could not be applied except to the northwest quadrant. This is due to range folding and/or low signal and the constraint that an analysis volume should be at least 28° wide. The analysis shows strong convergence ($\sim 10^{-3} \text{ s}^{-1}$) along the 270° radial, which coincides with the location of the storm complex. There is a large value of convergence at 305° , 38 km; this is probably due to ground clutter contamination of the radial velocities.

At 1847, more data is available for analysis. There is an area of divergence associated with the storm complex to the west, with only a small area of convergence ($-5 \times 10^{-4} \text{ s}^{-1}$) near the maximum reflectivity. The predominance of divergence is in qualitative agreement with the dissipation of the storm after 1847.¹² There is an area of small convergence ($-5 \times 10^{-4} \text{ s}^{-1}$) to the northwest and convective cells have developed here since 1732.

4.3 LINEARITY OF THE VELOCITY FIELDS

As noted earlier, with the presence of strong convection the assumption of spatial linearity is likely to be inaccurate. There are several techniques that can be applied to the residuals from the linear fit to assess the accuracy of the linear assumption.¹³ An easy and effective one is to plot the measured velocities v_r against the modeled velocities \hat{v}_r . Systematic deviations from linearity are then apparent on inspection of the plot.

A program RESIDUAL was written to produce plots of v_r vs \hat{v}_r using the NCAR graphics package. The residuals from the linear wind analysis were examined at 30° intervals, and a worst and best case are shown in Figures 12 and 13, respectively. Figure 12 is for an analysis at 1732 CST, $265^\circ/66.6 \text{ km}$, which is at the leading edge of the storm complex where a gust front is producing high shear values. Because the gust front is small compared to the analysis volume, the

12. Burgess, D.W. (1983) Personal communication.

13. Draper, N.R., and Smith, H. (1966) Applied Regression Analysis, John Wiley and Sons, New York, 407 pp.

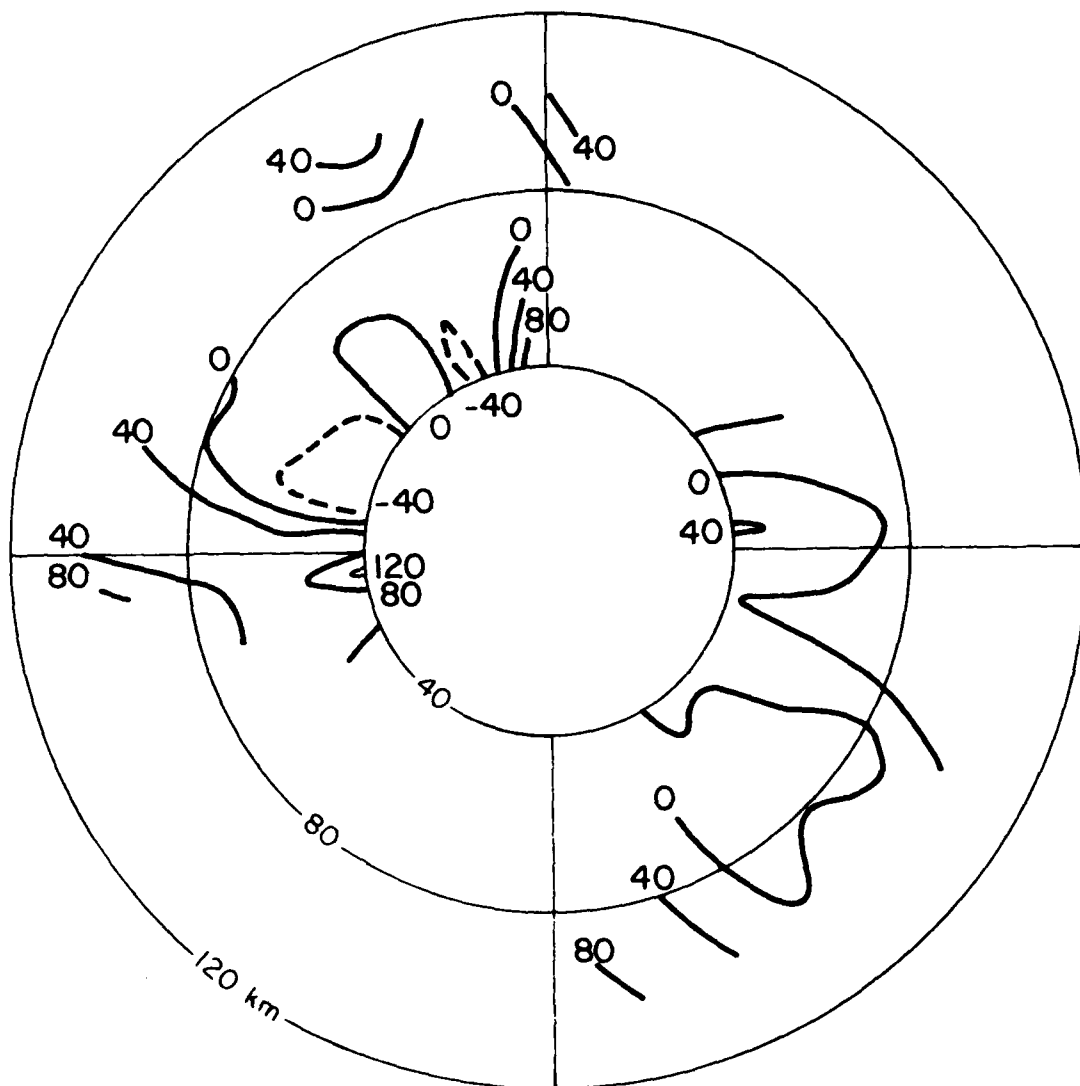


Figure 11. Divergence for 1847 CST.

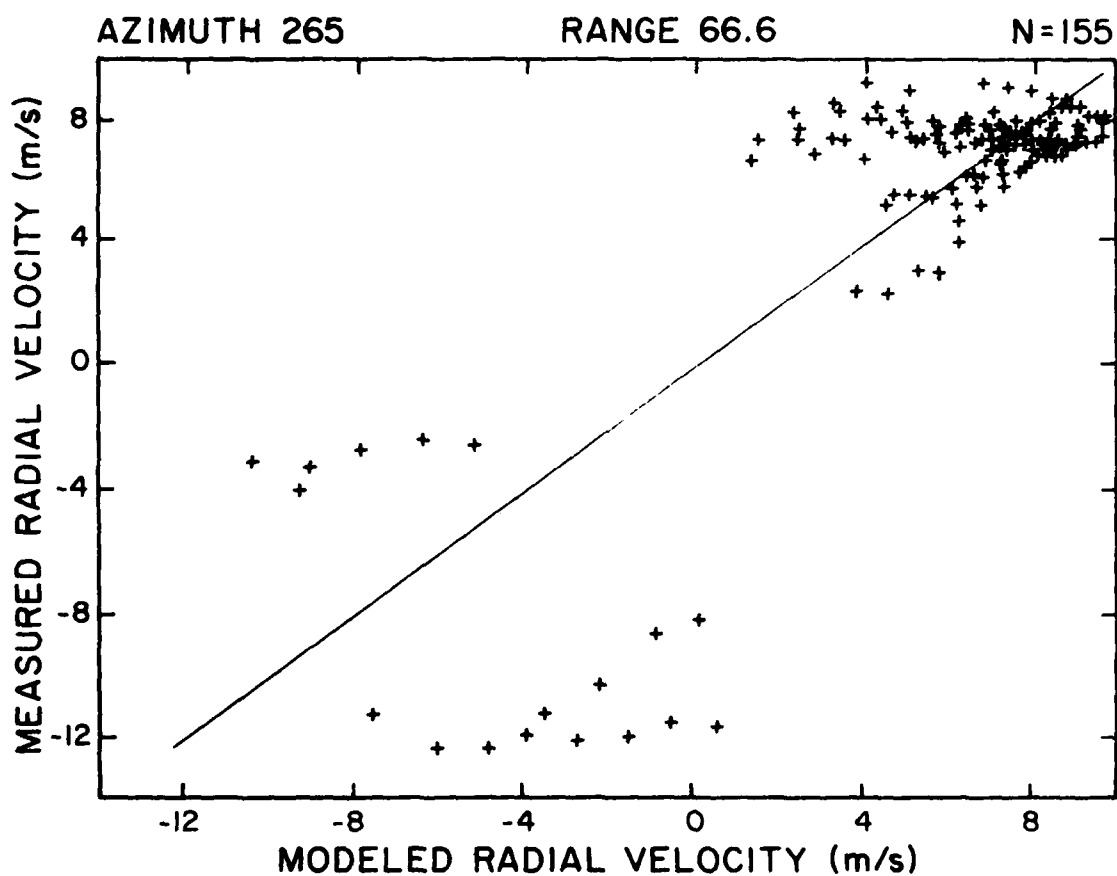


Figure 12. Radial velocity data for an analysis volume at 265°, 66.6 km for 1732. Measured radial velocity is plotted against the linearly modeled radial velocity, denoted by +. Solid line is a perfect linear relationship.

wind field deviates from linearity. In spite of the deviation, the linear analysis gives reasonable values of convergence (-10^{-3} s^{-1}).

Figure 13 is for 1732 CST, $285^\circ/42.3 \text{ km}$, which is northeast of the storm. The linear model fits very well here and the rms is small (0.36 m s^{-1}).

This plotting technique for testing the linearity assumption is sufficient for research purposes. For operational use, there would simply be too many plots to produce and examine. There are test statistics for adequacy of the linear model¹³ and further research in this area is needed.

5. SUMMARY AND CONCLUSIONS

An algorithm for linear wind field analysis suitable for real time application has been described. This algorithm uses range averaging over rather long ($\sim 7 \text{ km}$) intervals to reduce the number of computations needed. The use of linear wind analysis assumes the dominant spatial scales are large compared to the analysis volume and the averaging over range is consistent with this assumption.

A Fortran implementation (DIVERGE) of this algorithm has been described. DIVERGE is divided into data collection, analysis, and display segments. Only the data collection portion is under real time constraints. The program requires less than 300 kilobytes of memory and will execute in less than 10 minutes.

DIVERGE was applied to data from the Norman Doppler radar for April 9, 1978. Because of the convective nature of the precipitation, this data provides a severe test for the algorithm. The divergence measurements are consistent with other observations about the evolution of the storms. A technique for testing the linearity of the velocity field was used and further research recommended.

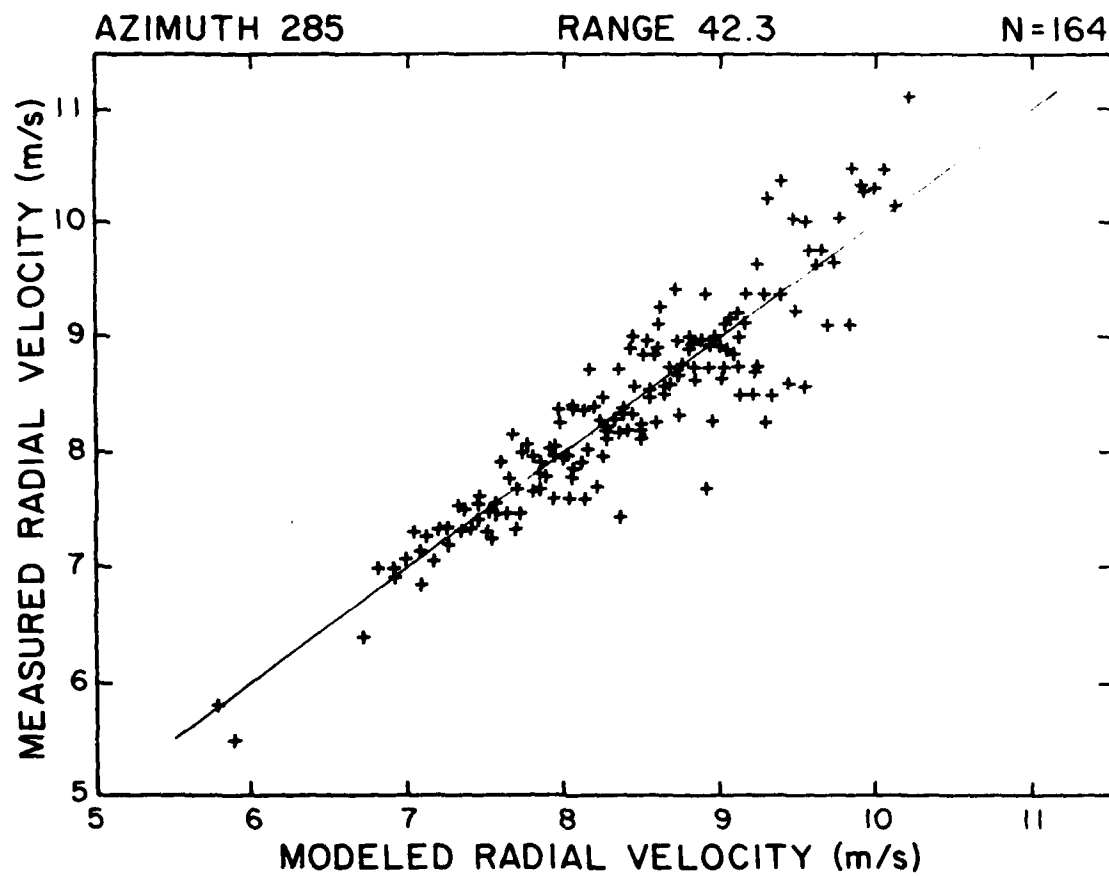


Figure 13. Same as Figure 12 but for 285°, 42.3 km.

References

1. Rabin, R., and Doviak, R.J. (1982) Prestorm observations in the clear air boundary layer with a Doppler radar. Preprints, 12th Conf. on Severe Local Storms, Amer. Meteor. Soc., Boston, Massachusetts, pp 425-429.
2. Chen, Chaing-Heins, and Orville, H.D. (1980) Effects of mesoscale convergence on cloud convection. J. Appl. Meteor. 19, pp 256-274.
3. Watson, A.I., and Holle, R.L. (1982) The relationship between low level convergence and convective precipitation in Illinois and South Florida. NOAA Tech. Rept. No. 7, ERL-OWRM, Boulder, Colorado, and Illinois State Water Survey, Champaign-Urbana, Illinois, 65 pp.
4. Ogura, Y., and Chen, Y. (1977) A life history of an intense mesoscale convective storm in Oklahoma. J. Atmos. Sci., 34, pp 1458-1476.
5. Ray, P.S. (1976) Vorticity and divergence fields within tornadic storms from dual-Doppler observations, J. Appl. Meteor., 15, pp 879-890.
6. Waldteufel, P., and Corbin, H. (1979) On the analysis of single Doppler data. J. Appl. Meteor., 18, pp 532-542.
7. Koscielny, A.J., Doviak, R.J., and Rabin, R. (1982) Statistical consideration in the estimation of divergence from single Doppler radar and application to prestorm boundary layer observations. J. Appl. Meteor., 21, pp 199-210.
8. Hennington, L. (1981) Reducing the effects of Doppler radar ambiguities. J. Appl. Meteor., 20, pp 1543-1546.
9. Akima, H. (1978) A method of bivariate interpolation and smooth surface fitting for irregularly distributed data points. ACM, Trans. on Math. Software., 4, pp 148-159.

References

10. McArthur, G.R. (1981) The SCD graphics utilities, NCAR Technical Note TN/166 +IA.
11. JDOP Staff (1979) Final report on the Joint Doppler Operational Project (JDOP), 1976-1978. NOAA Tech. Memo. ERL NSSL-86, 84 pp.
12. Burgess, W.W. (1983) Personal communication.
13. Draper, N.R., and Smith, H. (1966) Applied Regression Analysis, John Wiley and Sons, New York, 407 pp.

Appendix A

Effects of Applying a Linear Approximation to Sinusoidal Phenomena

Let $f(x) = A \cos(kx + \phi)$ represent the phenomena we are trying to model, where A is the amplitude, $k = 2\pi/L$ is the wave number, L is the wavelength, and ϕ is some arbitrary phase angle. $f(x)$ is approximated by a linear least square fit over the interval $-\frac{X}{2} \leq x \leq \frac{X}{2}$, as shown in Figure A.1. To least squares fit the line $a + kbx$, the quantity

$$F(k, x) = \int_{-\frac{X}{2}}^{\frac{X}{2}} [f(x) - (a + kbx)]^2 dx \quad A.1$$

is minimized. Setting the partials of F with respect to a and b to zero and solving gives

$$a = A \cos \phi \frac{\sin \pi \zeta}{\pi \zeta} \quad A.2$$

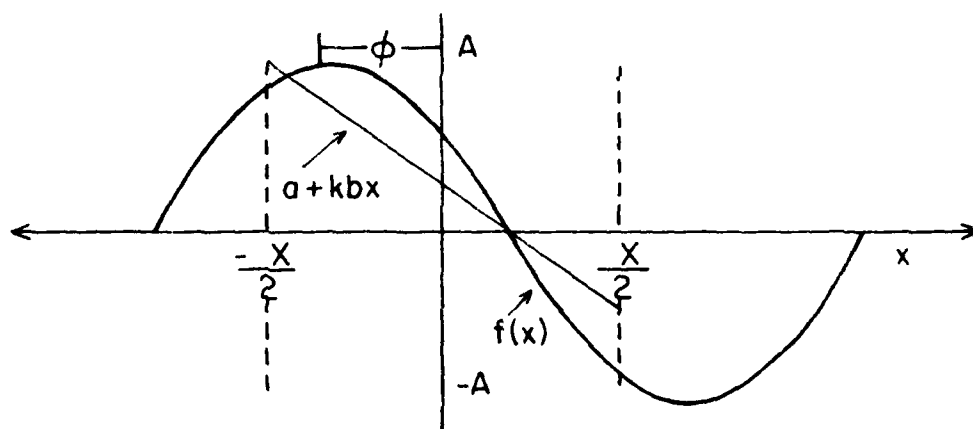


Figure A.1 Linear least squares approximation of a cosine wave.

$$kb = \frac{3 Ak \sin \phi}{(\pi \zeta)^3} [\pi \zeta \cos \pi \zeta - \sin \pi \zeta] \quad A.3$$

where $\zeta = \frac{x}{L}$ is the fraction of a wavelength that is being approximated.

The true derivative of $f(x)$ has a sinusoidal variation,

$$f_x = -Ak \sin(kx + \phi)$$

and its value at $x=0$ is $-Ak \sin \phi$.

Taking the ratio of kb to $f_x(x=0)$ gives

$$R(\zeta) \equiv \frac{kb}{f_x(x=0)} = \frac{3[\sin \pi \zeta - \pi \zeta \cos \pi \zeta]}{(\pi \zeta)^3} . \quad A.4$$

$R(\zeta)$ is shown in Figure A.2. For wave fractions less than 0.1, the least squares slope is a good representation of the first derivative. Between 0.1 and 1, the least squares slope is increasingly attenuated. For wave fraction greater than 1, there are negative lobes with the maximum amplitude of 0.08.

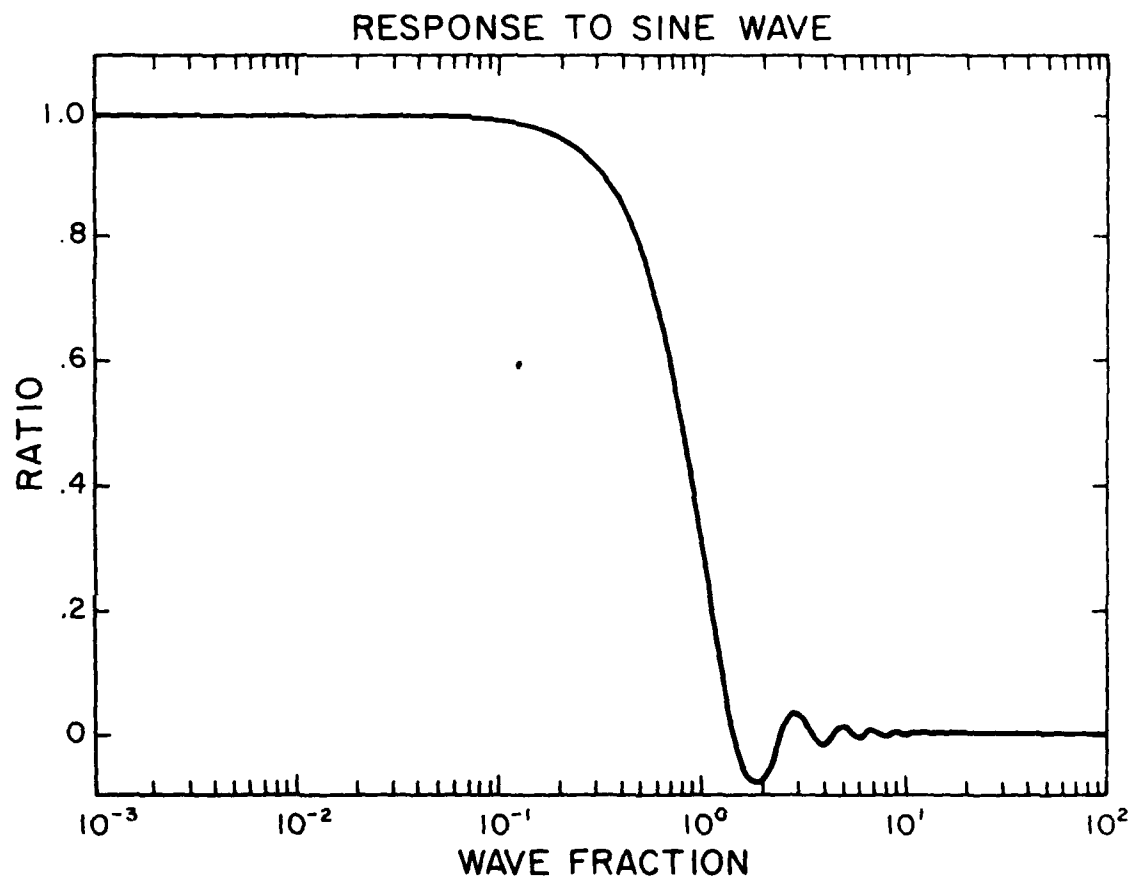


Figure A.2 Response of the least squares slope estimate to a sine wave. Wave fraction is the ratio of the fitting interval (X in Figure A.1) to the wavelength L .

Appendix B

Documentation for RLTDIV Subroutine

A	- (REAL, SCALAR)	x coordinate (meters) of analysis volume center.
AE	- (REAL, SCALAR)	4/3 earth radius in meters.
AMSVL	- (REAL, SCALAR)	missing value code - value larger in absolute value are missing.
AZ	- (REAL, SCALAR)	temporary azimuth, in radians.
AZC	- (REAL, SCALAR)	center azimuth in radians.
AZM	- (REAL, ARRAY)	azimuths of input data in degrees.
B	- (REAL, SCALAR)	y coordinate in meters of analysis volume center.
C	- (REAL, SCALAR)	z coordinate in meters of analysis volume center.
CENTER	- (REAL, ARRAY)	input center of analysis volume-azimuth (degrees), range (km), elevation (degrees).
COSPE	- (REAL, SCALAR)	cosine of elevation angle modified for earth's curvature.
COST	- (REAL, SCALAR)	cosine of current azimuth angle.
DET	- (D.P., SCALAR)	determinant of $P^t P$ matrix.
DGRD	- (REAL, SCALAR)	conversion for degrees radians.
DIV	- (REAL, SCALAR)	divergence measurement (s^{-1}).
EL	- (REAL, SCALAR)	current elevation angle in radians.
ELC	- (REAL, SCALAR)	center elevation angle in radians.
ELCE	- (REAL, SCALAR)	center elevation modified for earth curvature, in radians.
ELV	- (REAL, ARRAY)	elevation of input data in degrees.
ELVOLD	- (REAL, SCALAR)	last elevation angle processed, in radians.
EPS	- (REAL, SCALAR)	a small quantity.
GR	- (REAL, SCALAR)	ground range in meters.

I	- (INT2, SCALAR)	general purpose index
IRAD	- (INT2, SCALAR)	index for radials
IRNG	- (INT2, SCALAR)	index for range gates
IV	- (INT1, SCALAR)	index for input velocities
J	- (INT2, SCALAR)	general purpose index
K	- (INT2, SCALAR)	general purpose index
L	- (INT2, SCALAR)	general purpose index
MP	- (INA4, SCALAR)	number of parameter in linear wind model
NRAD	- (INA4, SCALAR)	number of radials in input data
NRNG	- (INA4, SCALAR)	number of range gates in input data
NV	- (INT1, SCALAR)	counter for good values of velocity
NVR	- (INT2, SCALAR)	total number of values in oVR
PARM	- (D.P., ARRAY)	parameters of linear wind field
PHIC	- (REAL, SCALAR)	earth curvature angle in radians
PHICO	- (REAL, SCALAR)	earth curvature angle for analysis volume center
PRED	- (REAL, ARRAY)	regressor variables
PTP	- (D.P., ARRAY)	sums of squares and cross products of regressor variables
PTV	- (D.P., ARRAY)	sum of cross products of regressor variables and radial velocities
RANGE	- (REAL, SCALAR)	range in meters
RGC	- (REAL, SCALAR)	range to center of analysis volume in meters
RMSERR	- (REAL, SCALAR)	root mean square of radial velocities about the linear model
RNG	- (REAL, ARRAY)	ranges for input data in km
RSQ	- (REAL, SCALAR)	r^2 statistic for significance of regression.
SINP	- (REAL, SCALAR)	sine of modified elevation angle
SNIPE	- (REAL, SCALAR)	dummy argument for statement function
SINT	- (REAL, SCALAR)	sine of azimuth angle
ST	- (REAL, SCALAR)	temporary store
STDDIV	- (REAL, SCALAR)	standard error of divergence measurement
STORE	- (REAL, SCALAR)	temporary store
SUM	- (D.P., SCALAR)	general summation
SUMMN	- (REAL, SCALAR)	summing location for r^2 calculation
SUMSQ	- (REAL, SCALAR)	summing location for r^2 calculation
VMAG	- (REAL, SCALAR)	typical value of radial velocity
VR	- (REAL, ARRAY)	input radial velocities, stored radial by radial
WORK	- (REAL, ARRAY)	work space of length MAX (9, NRNG)
DMINV	- (SUBROUTINE)	Double precision matrix inversion
HEIGHT	- (FUNCTION)	Height of radar beam for a 4/3 earth

FLOW CHART FOR RLTDIV SUBROUTINE

